International Journal of Current Engineering and Technology
E-ISSN 2277 – 4106, P-ISSN 2347 – 5161

Available at http://inpressco.com/category/ijcet

Research Article

A Study of Microstructures Characteristics of A356-Al_2O_3 Composites Produced by Cooling Slope and Conventional Stir Cast

Amir.A.Abdelsalam†*, T.S.Mahmoud‡, A.A.El-Betar† and A.M. El-Assal†

†Mechanical Engineering Department, Benha Faculty of Engineering, Benha University, Cairo, Egypt
‡Mechanical Engineering Department, Shoubra Faculty of Engineering, Benha University, Cairo, Egypt

Accepted 03 Nov 2015, Available online 08 Nov 2015, **Vol.5, No.6 (Dec 2015)**

Abstract

In this study, A356/Al_2O_3 metal matrix nano composites (MMNCs) were fabricated using two techniques, typically, stir casting (SC) technique and a combination of stir casting and cooling slope casting (SC/CSC) techniques and their microstructures characteristics were compared. The A356 Al alloy was reinforced with Al_2O_3 nanoparticles having the average size of 50 nm. The effect of the volume fraction of the Al_2O_3 nanoparticles on the microstructures characteristics of A356/ Al_2O_3 MMNCs fabricated using the aforementioned techniques were evaluated. The microstructure of the A356/ Al_2O_3 MMNCs was also investigated using scanning electron microscope (SEM) equipped with attachments for energy dispersive X-ray (EDX) spectroscopy. The results showed that the average grain size of samples fabricated using SC technique was lower than those fabricated using SC/CSC technique. However, the addition of water-cooling resulted in that the average grain size of samples fabricated using SC/CSC technique exhibited lower average size of the α-Al grains in comparison with those fabricated without water-cooling.

Keywords: *Metal Matrix Nano Composites, Stir casting, cooling slope casting, microstructures, nanoparticles.*

1. Introduction

Metal Matrix Composites (MMCs) are engineered combination of metal (Matrix) and hard particles (Reinforcements) to tailored properties. They have very light-weight, high strength, and stiffness and exhibit greater resistance to corrosion, oxidation and wear. Particulate MMCs have nearly isotropic properties when compared to long fibre reinforced composites. The mechanical behaviour of the composites depends on the matrix material composition, size, weight fraction of the reinforcement and the method utilized to manufacture the composites. The distribution of the reinforcement particles in the matrix alloy is influenced by several factors such as rheological behaviour of the matrix melt, the particle incorporation method, interaction of particles and the matrix before, during, and after mixing (Hashim, *et al*, 2002).

There are number of techniques available for producing Al-MMNCs, for example, powder metallurgy, in situ, pressure infiltration, squeeze, ultrasonic and stir casting (Mazahery and Ostadshabani, 2011). Stir casting, is a relatively simple route for fabrication of Al-MMNCs reinforced by ceramic particles. However, there are some problems associated with the quality of the MMNCs produced, such as poor wettability and heterogeneous distribution of the reinforcement material. The poor wettability is due to the surface tension of the molten alloy, the very large specific surface area of nanoparticles, and the high interfacial energy of reinforcements and presence of a gas layer on the ceramic particle surface (Akbari, *et al*, 2013).

Thixoforming and thixocasting are the semi-solid processing (SSP) technologies, which offer the ability to produce components that can meet the stringent requirements for automotive industry by combining the near-net-shape capabilities of die-casting and mechanical properties of forging. The parts produced by thixoforming techniques are reported to have substantially higher quality than die-castings and lower cost forgings (Taghavi and Ghassemi, 2009),(Hosseini, *et al*, 2012). However, a special ingot with thixotropic (non-dendritic) microstructure is required for thixoforming. Therefore, ingots that are not made specifically for thixoforming, i.e. not possessing the appropriate microstructures, cannot be used. Several commercial Al alloys such as A356 and A357 Al alloy were used as thixoforming materials (Birol, 2009). These alloys provide high fluidity and good castability and usually are used in fabrication of automobile components.

Cooling slope casting (CSC) is one of the new methods for applying shear stress to produce semi-

*Corresponding author: **Amir.A.Abdelsalam**

solid casting with globular structure. In this method, molten metal with a suitable superheat is cast into the mould after crossing the slope plate. Solid nucleation is formed because of contacting between the melt and slope plate and also heat transferring (Ahmadabadi, *et al*, 2008). The objective of this work is to investigate the microstructural characteristics in the alloy A365 Al alloy reinforced with nanoparticles of Al_2O_3 (A356/ Al_2O_3 MMNCs) by using: (1) the conventional stirring casting (SC) alone and (2) a combination of stir casting and cooling slope casting (SC/CSC) methods

2. Experimental Procedures

2.1. Materials

In this study, The A356 Al alloy was used as a matrix material. The nominal chemical composition of A356 Al alloy is listed in Table 1. While Aluminium oxide (Al2O3) ceramic nanoparticles were used as reinforcing agent. The Al_2O_3 nanoparticles. The properties of Al2O3 nanoparticles are listed in Table 2.

Table 1 Chemical composition of A356 Al alloy (wt.-%)

A356 Al alloy	
Si	7.38
Mg	0.279
Fe	0.149
Cu	0.00233
Mn	0.00293
Ti	0.1414
Al	Bal.

Table 2 Properties of the Al_2O_3 nanoparticles

Reinforcement type	γ- Al_2O_3
Average density (g/cm^3)	3.6
Young's Modulus (GPa)	380
Average particle size (nm)	50
Melting Point (^oC)	2045 ^oC
Vickers Hardness (HV) (GPa)	18-23

2.2. Fabrication of A356/Al_2O_3 MMNCs

The solidus and liquidus temperatures of the A356 alloy were estimated by differential scanning calorimeter (DSC) technique.

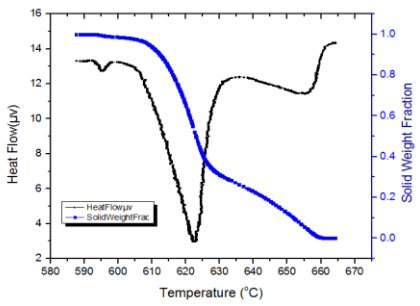

Fig. 1 DSC and solid fraction profiles within the semisolid temperature of the A356 alloy

The DSC approach directly measures the evolution of the heat of melting during the solid-liquid phase transformation. The solidus and liquidus temperatures of the A356 alloy were estimated by DSC to be 572°C and 617°C, respectively as shown in Fig.1. The Fig.1.shows also the solid fraction profiles within the semisolid temperature of the A356 alloy.

Fabrication of the A356/ Al_2O_3 MMNCs was carried out according to the following procedures: About 780 g of A356 Al alloy was melted at 680 ± 5 °C in a graphite crucible in an electrical resistance furnace. After complete melting and degassing by dry argon inert gas, Al foil capsules containing (0.5, 1 and 1.5 vol.-%) of Al_2O_3 nanoparticles were added manually into the A356 molten alloy. Mechanical stirring was used to produce the adequate homogenous Al_2O_3 nanoparticles distribution throughout the A356 matrix material. A stirrer with a diameter of 50 mm having four blades as shown in Fig. 2 was used. A stirring speed of about 1500 rpm was maintained throughout this work and the stirring time was about 1-3 minutes to achieve homogeneity of reinforcing particulates. For conventional stirring, after complete mixing of A356/ Al_2O_3 slurry, the agitation was stopped and the molten mixture was poured into preheated (≈ 200 ^oC) steel mould shown in Fig.3 made from tool steel and was allowed to cool to room temperature.

Fig. 2 The four blades mechanical stirrer

(a)

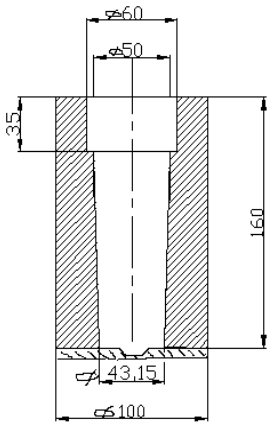

(b)

Fig. 3 The permanent steel mould; (a) a photograph, (b) a schematic illustration showing the dimensions of the mould (Dimensions in mm)

For cooling slope casting, the mixture was poured immediately after mechanical stirring on an inclined steel plate as in the cooling slope (CS) casting technique. The CS casting of the A356/ Al_2O_3 MMNCs involved pouring the molten mixture over an inclined cooling plate of 100 mm wide and 500 mm long. The cooling plate was made from low carbon steel. The cooling plate was fixed at 60o with respect to the horizontal plane and was cooled with water circulation underneath. Two different cooling conditions, typically with and without water-cooling were used during CS casting of A356/ Al_2O_3 MMNCs. The A356/ Al_2O_3 MMNCs was then poured in the same mould showing in Fig 3. The CS casting procedures of A356 /Al_2O_3 MMNCs is shown in Fig.4.

The cooling system includes a water pump, a water tank and coil water way devised between two steel plates. The flow rate of water was 23 liter/min and has a primary temperature of 25 ^oC. The water was pumped and circulated in the coil way as shown in Fig. 4. It is important to mention that, the surface of the inclined plate was coated with a thin layer of hard chrome in order to avoid sticking of the molten mixture on the slope and to facilitate a trouble-free melt flow.

2.3 Macro-And Microstructure Characterizations

Fig. 5 shows typical A356/ Al2O3 MMNCs ingot. The upper part of the ingots was removed as shown in Fig. 5. The remained part of the ingot was cut longitudinally into two parts and prepared for macrostructual examination. Metallographic samples were sectioned horizontally 5 mm from the top and bottom section of the remained parts of the ingots and then ground, and polished for microstructural examination as shown in Fig.5. After that, the specimens for microstructure examination were etched with Keller's reagent (2 ml HF (48%), 3 ml HCl, 5 ml HNO3 and 190 ml water) and the specimens for macrostructure examination were etched with Keller's reagent (20 ml HF (48%), 30 ml HCl, 50 ml HNO_3 and 190 ml water) . Keller's reagent is the most common etchant for Al and its alloys, except high Si alloys. The time of etching for each specimen was between 5-10 seconds. Microscopic examinations of the A356/ Al_2O_3 nano-particles composites and matrix alloy were carried out using an optical microscope equipped with digital camera.

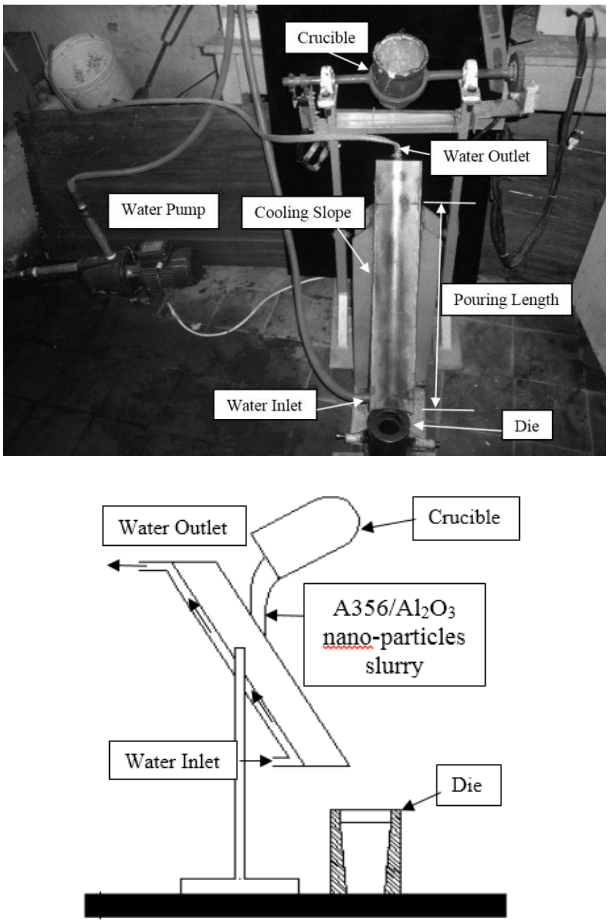

Fig. 4 Cooling slope casting apparatus used in the present work

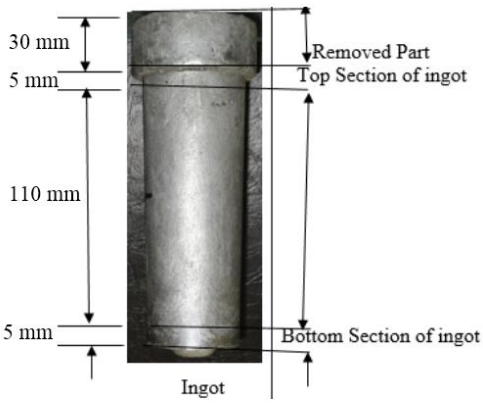

Fig. 5 A photograph shows a typical sample A356/Al_2O_3 MMNCs ingot and locations of the metallographic samples

The microstructures were characterized by measuring the particle size and shape of the primary α-Al grains by using Image analysis software. The particle diameter was determined using the following equation (Hosseini, *et al*, 2012):

$$d=2\times\sqrt{\frac{A}{\pi}} \quad (1)$$

Where d and A are the mean diameter and the area of the primary α-Al grains, respectively. The shape factor was calculated using the following equation (Hosseini,*et al*, 2012):

$$S.F.=\frac{4\pi A}{P^2} \quad (2)$$

Where S.F. is the shape factor, P is the perimeter of the α-Al grains, and A is the area of the α-Al grains. The ideal value of one for the shape factor shows that the particle is completely spheroid. The microstructure of the A356/ Al_2O_3 MMNCs was also investigated using scanning electron microscope (SEM) equipped with attachments for energy dispersive X-ray (EDX) spectroscopy and X-ray diffraction (XRD) analysis.

2.3 Porosity Measurements

In the present study, the actual or experimental density (ρ_{exp}) as well as the theoretical density (ρ_{th}) of the fabricated A356/ Al_2O_3 MMNCs were determined. The experimental density of the A356/ Al_2O_3 MMNCs was determined using the Archimedes' method according to ASTM B311-08 (Sajjadi, *et al*, 2012).

This method takes place by weighing test samples first in air and then in water. The A356/ Al_2O_3 MMNCs samples were precision weighed using an digital balance of ± 0.005 g accuracy. In order to obtain accurate measurement, water temperature was being considered to get the definite water density. The experimental density can be determined using the following equation (Sajjadi, *et al*, 2012):

$$\rho_{exp}=\left[\frac{W_a}{W_a-W_w}\right]\rho_{water} \quad (g/cm^3) \quad (3)$$

Where:
ρ_{exp}: is the experimental (actual) density (g/cm^3).
W_a: weight of specimen suspended in air (g).
W_w: weight of specimen suspended in water (g).
ρ_{water}: density of water (g/cm^3).

The theoretical density of the A356/Al_2O_3 MMNCs was calculated using the rule mixture. The rule of mixture can be expressed by the following equation (He, *et al*, 2008):

$$\rho_{th}=\rho_m V_m+\rho_r V_r \quad (g/cm^3) \quad (4)$$

Where:
ρ_{th}: is the theoretical density of the composite (g/cm^3).
ρ_m: is the density of the matrix (g/cm^3).
ρ_r: is the density of the reinforcement particles (g/cm^3).
V_m: is the volume fraction of the matrix (vol. %).
V_r: is the theoretical density of the reinforcement particles (vol. %).

In the theoretical density calculations, the values of the densities of the A356 matrix alloy and Al_2O_3 particles have the densities of 2.68 and 3.9 g/cm3, respectively. The porosity volume percent in the cast monolithic A356 Al alloy and A356/ Al_2O_3 MMNCs was determined by comparing the measured density with that of their theoretical density using the following equation:

$$\text{Porosity volume percent} = [1-\frac{\rho_{exp}}{\rho_{th}}]\times 100\ \% \quad (5)$$

3. Results and Discussion

3.1. Porosity of A356/Al_2O_3 MMNCs

Fig. 6 shows the variation of the bulk porosity of the A356/ Al_2O_3 MMNCs with the Al_2O_3 vol.-% of the nanoparticles at different fabrication techniques. Generally, it has been found that the A356/ Al_2O_3 MMNCs fabricated using SC or SC/CSC techniques exhibited higher porosity content when compared with the monolithic A356 matrix alloy processed under the same conditions. It has been found also that, in spite of the fabrication technique, increasing the volume fraction of the Al_2O_3 nanoparticles increases the bulk porosity of the A356/ Al_2O_3 MMNCs.

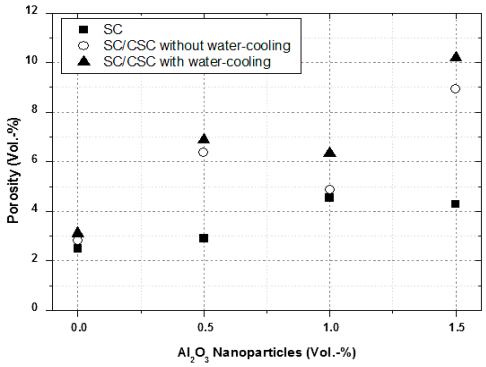

Fig.6 The variation of the porosity with the volume fraction of Al_2O_3 nanoparticles dispersed in A356/Al_2O_3 MMNCs fabricated using different techniques

The results revealed that the porosity of A356/Al_2O_3 MMNCs fabricated using stir casting (SC) was lower than those MMNCs fabricated using the combination of stir casting and cooling slope casting (SC/CSC) with and without water-cooling. However, the A356/Al_2O_3 MMNCs fabricated using SC/CSC technique with water-cooling exhibited higher porosity than those fabricated without water-cooling i.e. the introduction of cooling water has resulted in an increase in the porosity of A356/Al_2O_3 MMNCs.

For A356/Al_2O_3 MMNCs fabricated using SC technique, the increase of the porosity with the increase of the vol.-% of Al_2O_3 nanoparticles dispersed into the A356 Al matrix may attribute to the effect of low wettability and agglomeration at high content of reinforcements and pore nucleation at the matrix-Al_2O_3 interfaces. Moreover, decreasing liquid metal flow associated with the particle clusters leads to the formation of porosity. Such an observation has been reported by many workers (Mazahery and Ostadshabani,2011),(Sajjadi, *et al*, 2012),(Shabani and Mazahery, 2012), (Sajjadi, *et al*, 2012),(Mahallawi, *et al*, 2012).

In the present investigation, the introduction of cooling water during the fabrication of A356/Al_2O_3 MMNCs using SC/CSC technique increased the porosity content of the A356/Al_2O_3 MMNCs ingots. It is believed that the introduction of water-cooling has caused the molten A356/Al_2O_3 slurry to cool faster and increases its viscosity while flowing down the cooling slope Macrostructual Characteristics of MMNCs.

Figs. 7, 8, and 9 shows typical macrograph of the longitudinal cross-section of ingots produced using different fabrication conditions. It is clear that small size pores were observed large size pores were observed, especially, at the upper part of the A356/Al2O3 MMNCs ingots produced using both SC (For example, see Fig. 7 at 1 vol.-% Nano-particles ratio) and SC/CSC (For example, see Fig. 8 and Fig.9) techniques. The A356/Al2O3 MMNCs ingots produced using mechanical SC technique showed lower size and quantity of the pores than those ingots produced using SC/CSC technique with and without water-cooling. From Fig. 9, it clear that A356/Al2O3 MMNCs ingots produced using SC/CSC technique with water-cooling showed larger size and quantity of the pores than A356/Al2O3 MMNCs ingots produced using SC/CSC technique without water-cooling (see Fig.8). Figs. 8 and 9 shows also that increasing the Al2O3 nanoparticles content increasing the quantity of the pores of A356/Al_2O_3 MMNCs ingots.

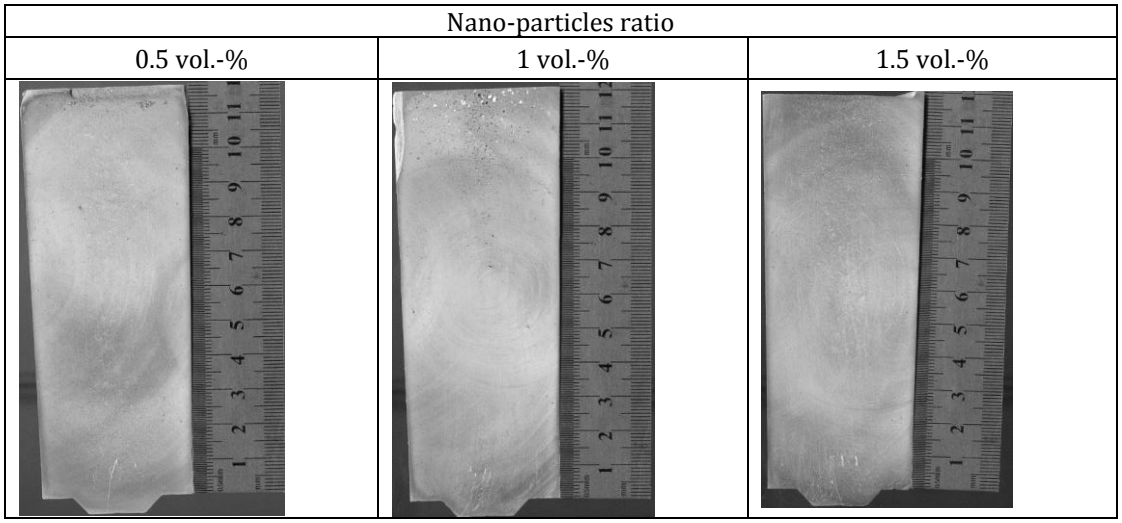

Fig. 7 Macrograph of the longitudinal cross-section of A356/Al_2O_3 MMNCs ingots produced using mechanical stirring casting (SC)

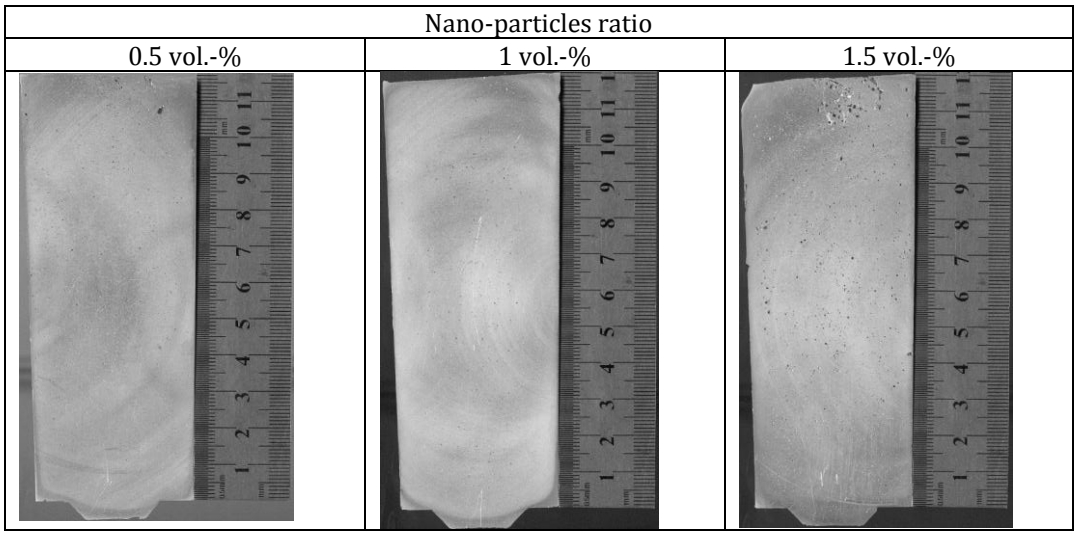

Fig. 8 Macrograph of the longitudinal cross-section of A356/Al_2O_3 MMNCs ingots produced using SC/CSC technique without water-cooling

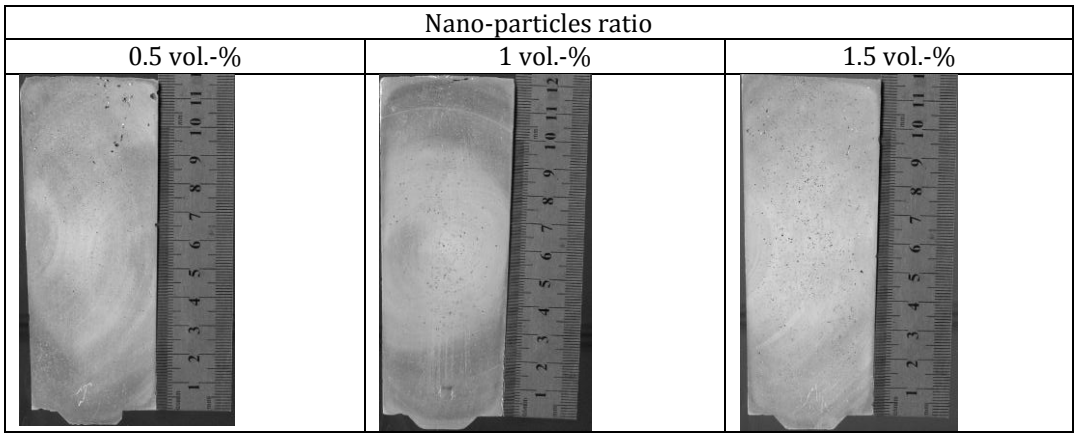

Fig. 9 Macrograph of the longitudinal cross-section of A356/Al_2O_3 MMNCs ingots produced using SC/CSC technique with water-cooling

3.3 Microstructural Characteristics of MMNCs

The microstructure of the conventionally cast A356 monolithic alloy has typical dendritic structure (see Fig. 10). Large dendrites of α-Al grains with size more than 100 μm were observed. It is clear from Fig. 10 that the structure of the monolithic A356 Al alloy consists mainly of the primary α-Al dendrites (white regions) and the eutectic mixture composed of α-Al and Si (darker regions). Needle-like primary Si particulates were distributed along the boundaries of the α-Al dendrites. Figs. 11 to 15 shows the microstructure of A356 monolithic alloy as well as A356/Al_2O_3 MMNCs ingots produced using different fabrication techniques. It is clear that the microstructure of the A356 alloy is completely different. The CS cast ingots showed non-dendritic microstructure of the primary α-Al phase.

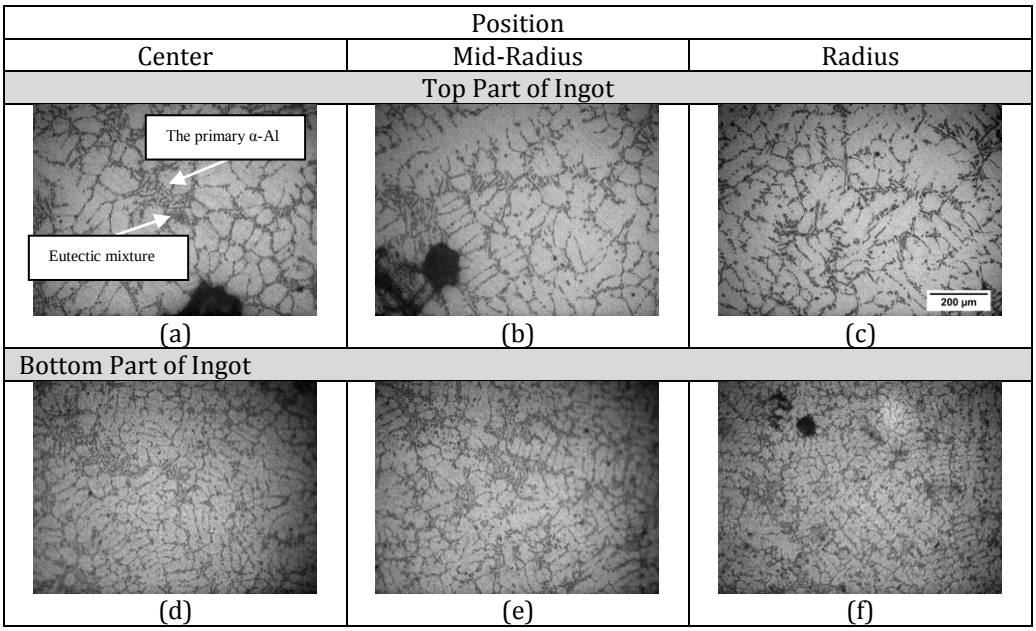

Fig. 10 Microstructures of the conventionally cast A356 monolithic alloy

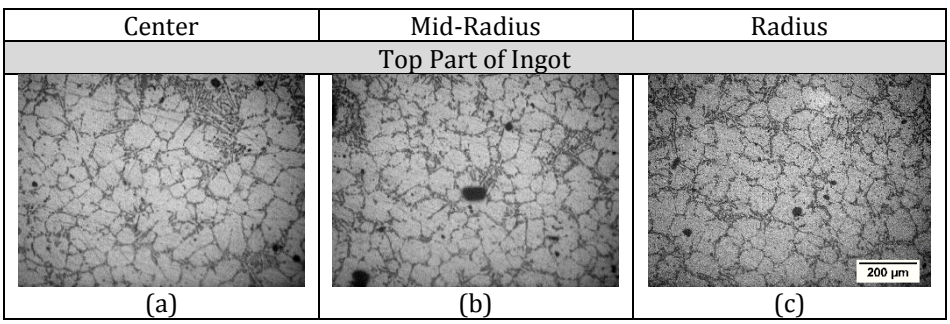

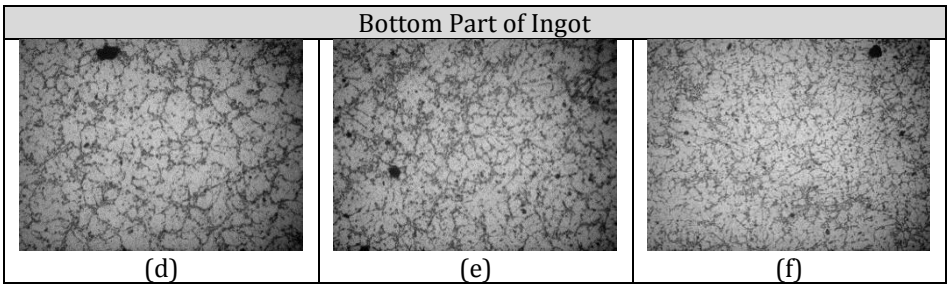

Fig. 11 Microstructures of A356 monolithic alloy ingot produced using cooling slope casting without water-cooling

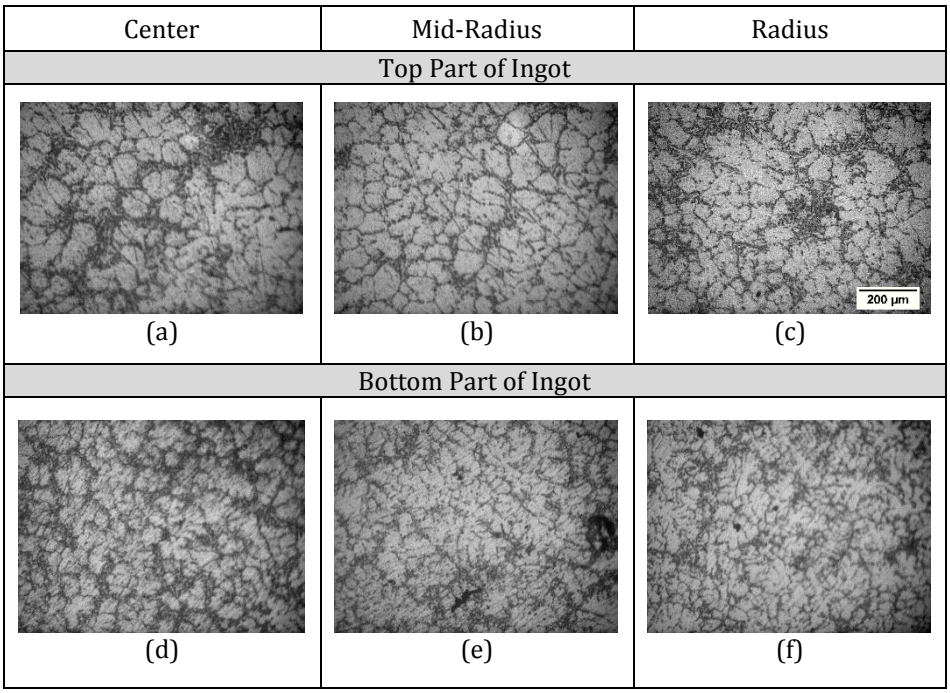

Fig. 12 Microstructures of A356 monolithic alloy ingot produced using cooling slope casting with water-cooling

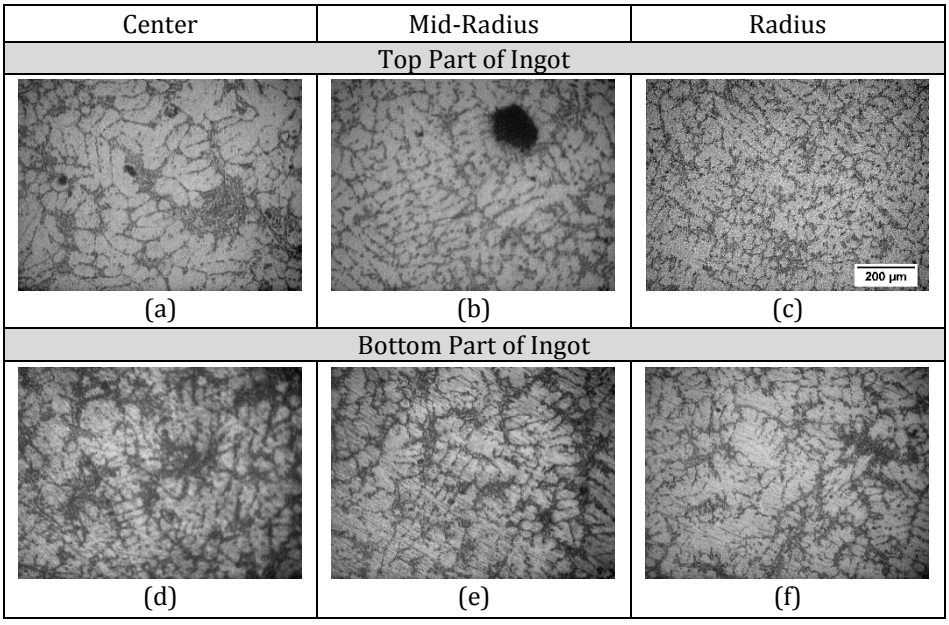

Fig. 13 Microstructures of A356/1.5 vol.-%Al_2O_3 MMNCs ingot produced using mechanical stirring casting technique

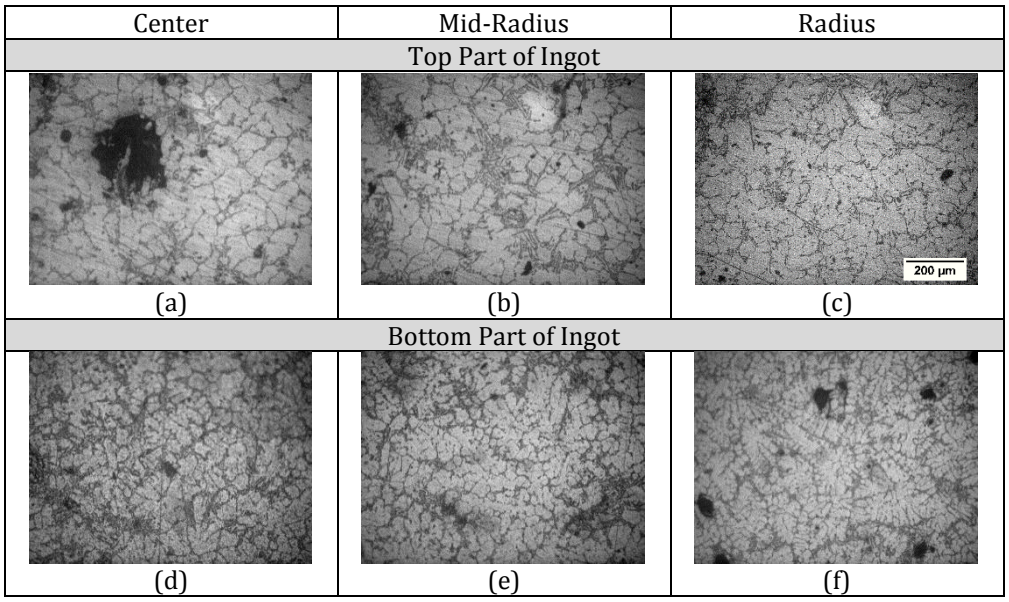

Fig. 14 Microstructures of A356/1.5 vol.-%Al_2O_3 MMNCs ingot produced using SC/CSC technique without water-cooling

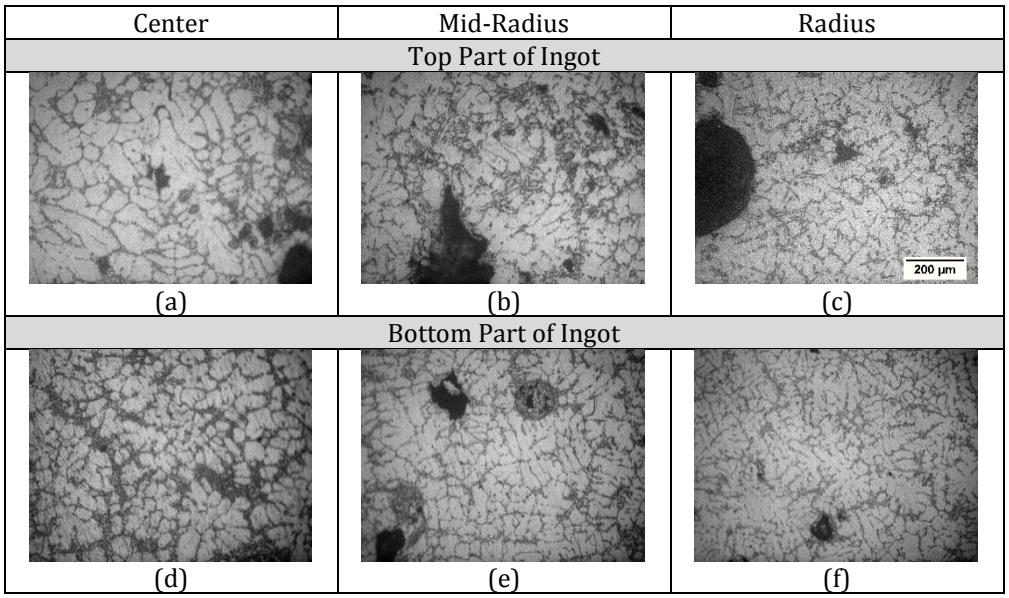

Fig. 15 Microstructures of A356/1.5 vol.-%Al_2O_3 MMNCs ingot produced using SC/CSC technique with water-cooling

Figs. 16 and 17 show the size and shape factor of the primary α-Al phase, respectively, at the top and bottom of A356 Al alloy ingots fabricated by different CSC techniques. It can be seen from Fig. 24 that finer α-Al grain obtained at the bottom than the top of the ingots. Also, the radius of the ingots exhibited the lowest grain sizes than the mid-radius and center of ingots. While the center of the ingots exhibited the largest grain sizes than the radius and mid-radius of ingots. It is believed that the finer grains of the edge were obtained because of its higher heat loss through the mould wall. Moreover, it has been observed that the A356 Al alloy ingots produced using cooling slope casting with water-cooling exhibited lower grain size than those produced without water-cooling.

It is worth to note that the obtained result in this research is in agreement with the other researchers reported in the literature (Ghavamodini, *et al*, 2012), (Budiman, *et al*, 2009), (Legoretta, *et al*, 2008), (Budiman, *et al*, 2011).

The introduction of water-cooling reduced the size of the primary α-Al grains of the CS cast ingots. It is believed that the introduction of water-cooling has caused the molten metal to cool faster while flowing down the cooling slope. In solidification process, the nucleation and spherodisation can be influenced by cooling rate. Increasing the cooling rate can promote the nucleation rate. The change of the nucleation rate influences the grain size and the shape factor of the

primary α-Al grains. In the case of pouring without water-cooling, the number of crystals nucleated and detached from the surface of the cooling plate was insufficient to produce fine and spheroidal primary crystals.

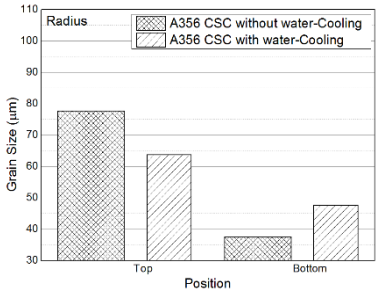

(a)

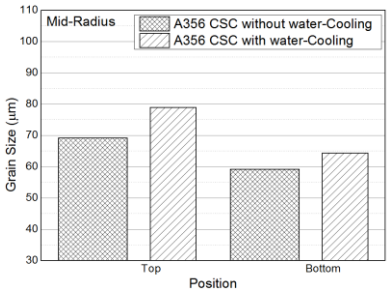

(b)

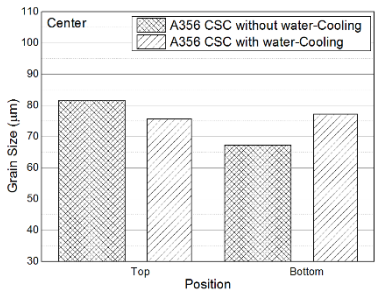

(c)

Fig. 16 The size of primary α-Al grains at top and bottom of A356 ingots and at the (a) radius, (b) mid-radius and (c) center of the CSC ingots

The introduction to water-cooling leads to higher fractional solidification on the cooling plate and increase the rate of nucleation and detachment of the α-Al crystals resulted in finer and non-dendritic primary α-Al grains. High pouring temperature leads to decreasing nucleation, remelting the primary crystals and undesired grain growth. Low pouring temperature causes rapid solidification of melt on the slope and thus dendritic solidification. In the present study, the effect of water cooling on the shape factor is not noticeable (see Fig. 17). The ingots CSC with and without water-cooling exhibited shape factor ranges between ~0.7 and ~0.8. Fig. 18 and 19 show the variation of the average grain size (average of bottom and top) and average shape factor, respectively, of the primary α-Al phase with the volume fraction of Al_2O_3 nanoparticles dispersed in A356/Al_2O_3 MMNCs fabricated using different techniques.

The results revealed that A356/Al_2O_3 MMNCs produced using SC technique exhibited lower α-Al grain size than those fabricated using SC/CSC techniques. However, the introduction of water-cooling during the fabrication of A356/Al_2O_3 MMNCs using SC/CSC technique assisted in reducing the average size of the α-Al grains. In general, increasing the volume fraction of the Al_2O_3 nanoparticles up to 1 vol.-% reduces the average grain size of the A356/Al_2O_3 MMNCs. In most cases, increasing the volume fraction of the Al_2O_3 nanoparticles above 1 vol.-% (i.e. 1.5) tends to increase the average size of the α-Al grains.

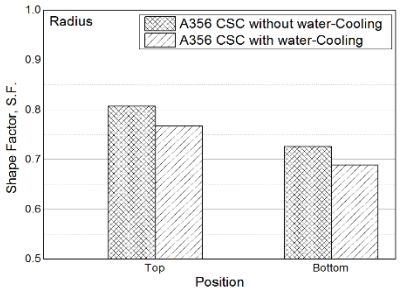

(a)

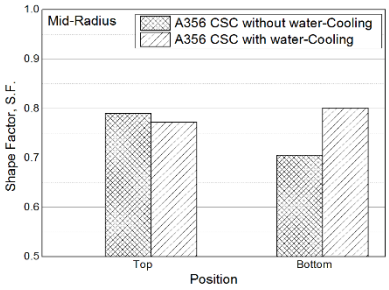

(b)

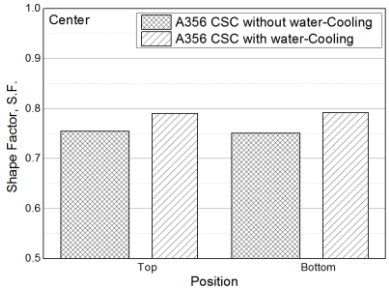

(c)

Fig. 17 The shape factor of primary α-Al grains at top and bottom of A356 ingots and at the (a) radius, (b) mid-radius and (c) center of the CSC ingots

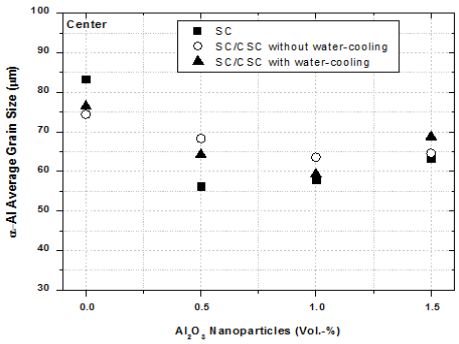

(a)

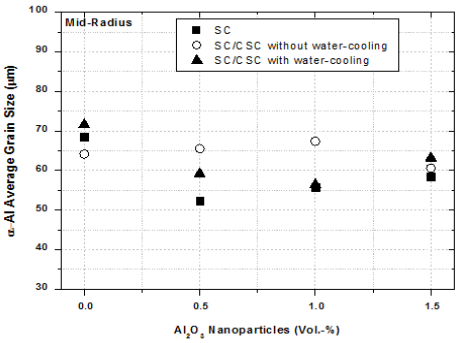

(b)

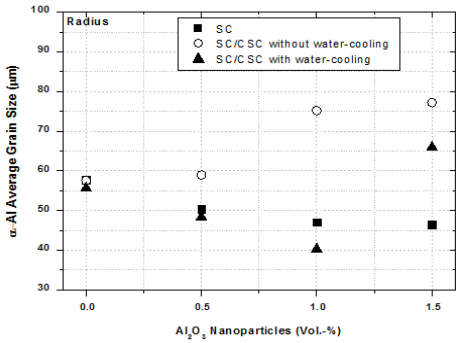

(c)

Fig. 18 The variation of the average grain size of the primary α-Al phase with the volume fraction of Al_2O_3 nanoparticles dispersed in A356/Al_2O_3 MMNCs fabricated using different techniques

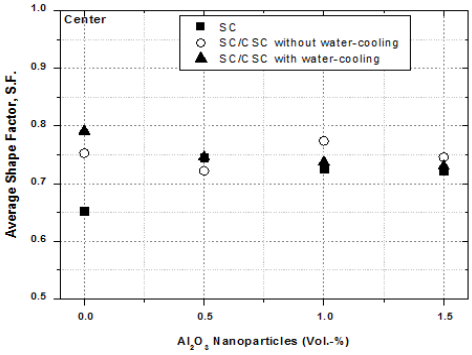

(a)

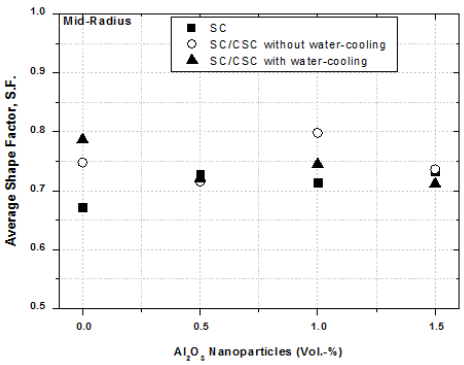

(b)

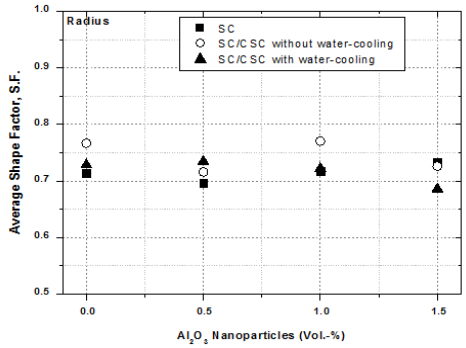

(c)

Fig. 19 The variation of the average shape factor of the primary α-Al phase with the volume fraction of Al_2O_3 nanoparticles dispersed in A356/Al_2O_3 MMNCs fabricated using different techniques

Water-cooling was introduced as the parameter that caused the molten alloy to cool faster and increase in fractional solidification while flowing down the cooling plate. In solidification process at cooling slope, the increase in cooling rate can promote the nucleation rate. The change of nucleation rate, on the other hand, can influence the grain size, shape factor and volume fraction of liquid or solid. For the pouring condition without water-cooling, the fraction of solid phase and as the result the number of crystals nucleated and detached from the surface of the cooling plate were insufficient to produce fine and spheroidal primary crystals.

But the addition of cooling system leads to higher fractional solidification that occurs on the cooling plate, so it would help to increase the rate of nucleation and detachment of α-Al grains. Consequently, degeneration of the dendritic structure advances and the microstructure is replaced by finer primary α-Al particles (Ghavamodini, *et al*, 2012). The results obtained from the present work revealed that the addition of the Al_2O_3 nanoparticles did not significantly influenced the shape factor of the primary α-Al grains. Increasing the Al_2O_3 volume fraction has little or no effect on the shape factor (see Fig. 19). Both of the A356 monolithic alloy and the A356/Al_2O_3 MMNCs exhibited practically the same shape factor.

As stated previously, the specimens produced by SC/CSC have larger size of α-Al grains compares to samples obtained from the SC. During SC, stirring the melt has three effects on the microstructure of composite samples: at first it causes to break the dendrite shaped structure and leave the structure in equiaxed form (Sajjadi, *et al*, 2011); second, it improves the wettability and incorporation of particles within the melt; and third it causes to disperse the particles more uniformly in the matrix.

Fig. 20 shows SEM micrographs of the microstructure of A356/Al_2O_3 MMNCs fabricated using SC technique. Figs. 21 and 22 show SEM micrographs of the microstructure of A356/Al_2O_3 MMNCs fabricated using SC/CSC technique without and with water-cooling, respectively. The round small white particles shown in the micrographs indicate the Al_2O_3 nanoparticulates. Agglomeration of such particulates may be found, especially, at higher volume fractions of Al_2O_3 nanoparticulates (For example see Fig. 21c).

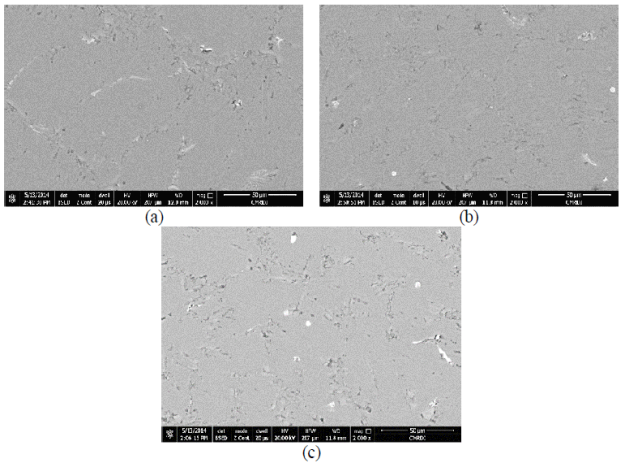

Fig. 20 SEM micrographs of A356/Al_2O_3 MMNCs with (a) 0.5 vol.-%, (b) 1 vol.-%, (c) 1.5 vol.% and fabricated using SC technique (50µm)

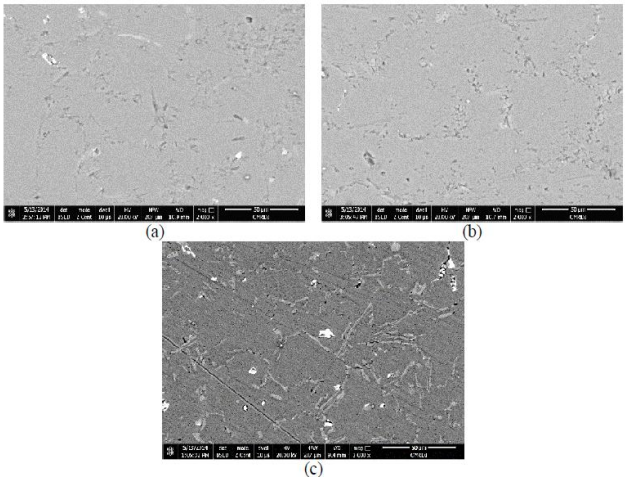

Fig. 21 SEM micrographs of A356/Al_2O_3 MMNCs with (a) 0.5 vol.-%, (b) 1 vol.-%, (c) 1.5 vol.% and fabricated using SC/CSC technique without water-cooling (50µm)

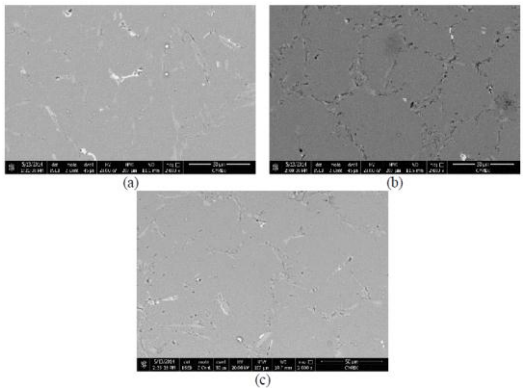

Fig. 22 SEM micrographs of A356/Al_2O_3 MMNCs with (a) 0.5 vol.-%, (b) 1 vol.-%, (c) 1.5 vol.% and fabricated using SC/CSC technique with water-cooling (50µm)

Fig. 23(a) shows high magnification SEM micrographs of the A356/1.5 vol. % Al_2O_3 MMNCs fabricated using SC/CSC technique without water-cooling, it will be also shown in Fig.23 (a) that the Al_2O_3 nano-particulates have a tendency to segregate and agglomerate at pores resulting from solidification shrinkage. The XRD analysis for the nanoparticles is shown in Fig.23 (b) indicates the presence of Al_2O_3 nano-particulates near the eutectic structure. Also, it has been observed that increasing the volume fraction of the nano-particlutes dispersed inside the A356 alloy increases the agglomeration percent.

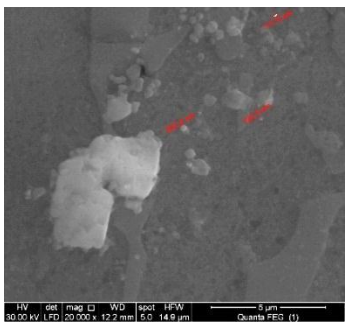

(a)

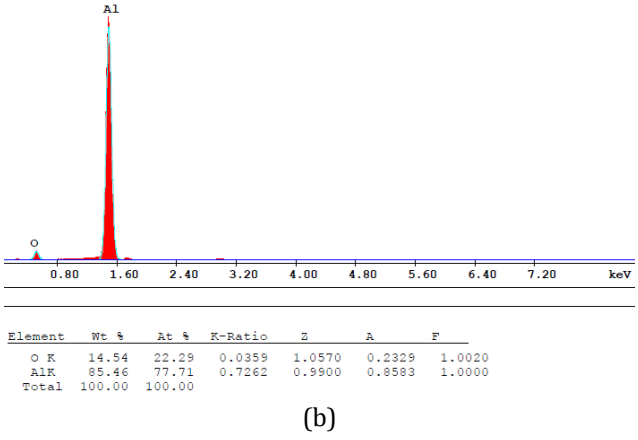

(b)

Fig. 23(a) shows high magnification SEM micrographs of the A356/1.5 vol. % Al_2O_3 MMNCs fabricated using SC/CSC technique without water-cooling. (b) XRD analysis for the particles shown in (a)

Conclusions

The following conclusions can be drawn from the current investigation:

1. The A356/Al_2O_3 MMNCs fabricated using stir casting (SC) or the combination of stir casting and cooling slope casting (SC/CSC) exhibited higher porosity content when compared with the monolithic A356 Al alloy.
2. For the different fabricated methods, increasing the volume fraction of the Al_2O_3 nanoparticles increases the porosity of the A356/Al_2O_3 MMNCs.
3. The porosity of A356/Al_2O_3 MMNCs fabricated using SC was lower than those fabricated using SC/CSC technique. The A356/Al_2O_3 MMNCs fabricated using SC/CSC technique with water-cooling exhibited higher porosity than those fabricated without water-cooling.
4. The A356/Al_2O_3 MMNCs ingots produced by both SC and SC/CSC showed non-dendritic microstructure of the primary α-Al phase. Finer α-Al grain obtained at the bottom than the top of the ingots. While, the radius of the ingots exhibited the lowest grain sizes than the mid-radius and center of ingots.
5. The A356/Al_2O_3 MMNCs produced using SC technique exhibited lower α-Al grain size than those fabricated using SC/CSC techniques. The introduction of water-cooling during the fabrication of A356/Al_2O_3 MMNCs using SC/CSC technique assisted in reducing the average size of the α-Al grains.
6. For A356/Al_2O_3 MMNCs ingots produced both SC and SC/CSC techniques, increasing the volume fraction of the Al_2O_3 nanoparticles up to 1 vol.-% reduces the average grain size of the A356/Al_2O_3 MMNCs. In most cases, increasing the volume fraction of the Al_2O_3 nanoparticles above 1 vol.-% (i.e. 1.5) tends to increase the average size of the α-Al grains.
7. The addition of the Al_2O_3 nanoparticles did not significantly influenced the shape factor of the primary α-Al grains. Increasing the Al_2O_3 volume fraction has little or no effect on the shape factor. Both of the A356 monolithic alloy and the A356/Al_2O_3 MMNCs exhibited practically the same shape factor.

Acknowledgments

The authors are thankful to Benha University .Benha and Shoubra Faculty of Engineering for providing financial support and facilities for carrying out this work.

References

J. Hashim, L. Looney and M.S.J. Hashmi, (2002), Particle Distribution in Metal Matrix Composites, Part-I, Journal of Materials Processing Technology, Vol.123, pp.251-257.

Ali Mazahery and Mohsen Ostadshabani, (2011), Investigation on Mechanical Properties of Nano-Al_2O_3-Reinforced Aluminum Matrix Composites, Journal of Composite Materials, Vol. 0, No.0, pp. 1–8.

M. Karbalaei Akbari, O. Mirzaee and H.R. Baharvandi, (2013), Fabrication And Study On Mechanical Properties And Fracture Behavior Of Nanometric Al_2O_3 Particle-Reinforced A356 Composites Focusing On The Parameters Of Vortex Method, materials and design, Vol. 46, pp. 199–205.

Farshid Taghavi and Ali Ghassemi, (2009), Study on the Effects of The Length and Angle of Inclined Plate on the Thixotropic Microstructure of A356 aluminum alloy, Materials and Design, Vol. 30, pp. 1762–1767.

S.S. Hosseini, S. Nourouzi, S.J. Hosseinipour and A. Kolahdooz, (2012), Effect Of Slope Plate Variable and Pouring Temperature On Semi-solid Microstructure of A356 Aluminum Alloy, Metal Forming.

Yucel Birol, "Semi-solid processing of the primary Aluminum die casting alloy A365, (2009), Journal of Alloys and Compounds, Vol. 473, pp. 133–138.

M. Nili-Ahmadabadi, F. Pahlevani, and P. Babaghorbani, (2008), Effect of Slope Plate Variable and Reheating on the Semi-Solid Structure of Ductile Cast Iron, Tsinghua Science And Technology, Vol. 13, pp. 147–151.

S.A. Sajjadi, M.T. Parizi, H.R. Ezatpour, A. Sedghi; (2012), Fabrication of A356 composite reinforced with micro and nano Al_2O_3 particles by a developed compocasting method and study of its properties, Journal of Alloys and Compounds, , Vol. 511, pp. 226–231.

He, Y., Xing, S., Xie, S., Huang, G., Gou, J., (2008), Microstructure and thermal plasticity of semi-solid M2 steel casting ingots using inclined slope pre-crystallization method", In: Proceedings of the 10th International Conference on the Semi-Solid Processing of Alloys and Composites, pp. 539–544.

Mohsen Ostad Shabani and Ali Mazahery, (2012), Aluminum-matrix nanocomposites: swarm-intelligence optimization of the microstructure and mechanical properties, materials and technology, Vol. 46, pp. 613–619.

S.A. Sajjadi, H.R. Ezatpour, and M. Torabi Parizi, (2012), Comparison of microstructure and mechanical properties of A356 aluminum alloy/ Al_2O_3 composites fabricated by stir and compo-casting processes, Materials and Design, Vol. 34, pp. 106–111.

I.El-Mahallawi, H.Abdelkader, L.Yousef, A.Amer, J.Mayer, and A.Schwedt, (2012), Influence of Al_2O_3 nano-dispersions on microstructure features and mechanical properties of cast and T6 heat-treated AlSi hypoeutectic Alloys, Materials Science &Engineering, Vol.556 A, pp. 76–87.

S.M. Ghavamodini, S. Nourouzi , H. Baseri, and A. Kolahdooz, (2012), Effect of casting temperature and cooling system on the microstructure of Al-A356 feedstock produced by cooling slope method, Metal Forming.

H. Budiman, M.Z. Omar, A. Jalar, and A.G. Jaharah, (2009), Effect of Water Cooling on the Production of Al-Si Thixotropic Feedstock by Cooling Slope Casting, European Journal of Scientific Research, Vol. 32, pp.158-166.

E. Cardoso Legoretta, H. V. Atkinson, H. Jones, (2008), Cooling slope casting to obtain thixotropic feedstock II: observations with A356 alloy, Journal of Material science, Vol. 43, pp. 5456–5469.

H. Budiman, M. Z. Omar, A. Jalar and J. Syarif, (2011), Investigation on Cooling Slope and Conventional Stir Cast A356/ Al_2O_3 Metal Matrix Composites, Advanced Materials Research, Vol. 154-155, pp. 1284-1287.

S.A. Sajjadi, H.R. Ezatpour, H. Beygi, (2011), microstructure and mechanical properties of Al– Al_2O_3 micro and nanocomposites fabricated by stir casting," materials science and engineering a, Vol. 528, pp. 8765–8771.